Egyptian Journal of Chemistry

http://ejchem.journals.ekb.eg/

Enhancing the Optical Properties of Starch/ZnO Nanocomposite Using Graphene Oxide

Rania Badry[1], Maroof A. Hegazy[2], Ibrahim S. Yahia[3-5], Hanan Elhaes[1], Heba Y. Zahran[3-5], Ahmed I. Abdel-Salam[6], Hanan Matar[6] and <u>**Medhat A. Ibrahim**</u>**[6-7]***

[1]*Physics Department, Faculty of Women for Arts, Science and Education, Ain Shams University, 11757 Cairo, Egypt;*
[2]*National Research Institute of Astronomy and Geophysics (NRIAG), 11421 Helwan, Cairo, Egypt*
[3]*Research Center for Advanced Materials Science (RCAMS), King Khalid University, Abha 61413, P.O. Box 9004, Saudi Arabia.*
[4] *Laboratory of Nano-Smart Materials for Science and Technology (LNSMST), Department of Physics, Faculty of Science, King Khalid University, P.O. Box 9004, Abha, Saudi Arabia.*
[5]*Nanoscience Laboratory for Environmental and Bio-Medical Applications (NLEBA), Semiconductor Lab., Metallurgical Lab.1., Physics Department, Faculty of Education, Ain Shams University, Roxy, 11757 Cairo, Egypt.*
[6]*Nanotechnology Research Centre (NTRC), The British University in Egypt (BUE), Suez Desert Road, El-Sherouk City, Cairo, 11837, Egypt.*
[7]*Molecular Spectroscopy and Modeling Unit, Spectroscopy Department, National Research Centre, 33 El-Bohouth St., 12622, Dokki, Giza, Egypt.*

Abstract

Due to its biocompatibility, starch is an eco-friendly polymer for various applications, from medical applications to optoelectronic ones. Polymer nanocomposites based on starch, zinc oxide nanoparticles (ZnO NPs), and graphene oxide (GO) are synthesized using a casting technique. A UV-Vis spectrophotometer studied optical properties, and the nanocomposite molecular structure was determined using a Fourier transform infrared (FTIR) spectrometer. The starch absorption edge was shifted to the lower energy region, and it was found that starch has two absorption edges and hence two optical band gaps. The direct and indirect optical band gap values were determined for pure starch, starch/ZnO, and starch/GO nanocomposites. Incorporating 6wt.% of ZnO NPs reduces the indirect optical bandgap from 4.77 to 2.88 eV. Meanwhile, incorporating 2wt.% of GO reduced the bandgap to 2.15 eV.

Keywords: Starch; Zinc oxide; GO and UV-Vis Spectrophotometer.

1. Introduction

Human life is completely determined by machine-driven systems supported by advanced materials with new functionality in the current era. Various synthetic approaches are applied to develop man-made materials for quality improvement in life [1]. Similarly, biomaterials made from renewable raw materials are also easy-to-use substances. They are considered perfect for applications in numerous research areas such as biotechnology, optoelectronics, and energy storage devices [2]. Materials obtained naturally are considered sustainable without major efficiency losses and are abundant [3]. Starch is a biomaterial derived from nature and has attracted many advanced

applications by connecting both the physico-chemical advantages and functional properties aided by reactive groups containing oxygen. Starch, in the form of granules, consists of various glucose molecules linked by glycosidic bonds [4]. The starch granules' properties such as structure, size, and chemical composition depend on the initial state from which they are extracted. Starch contains two macromolecules, namely amylose and amylopectin, that form the basic signature. Amylose appears as a linear structure made up of linked 1,4-glucose units, while the amylopectin structure is a highly branched one with 1,4-chains [5]. Starch, which belongs to the group of polysaccharides, is suitable for the development of food packaging substances because of its environmentally pleasant nature, transparency, flexibility, thermoplastic nature, and affordability.

Energy storage as a biopolymer is very common in nature. Green plants and algae store starch for energy. Starch is a major source of calories in human food, both direct and indirect. The first is achieved through the consumption of plant products, and the second is when used as animal feed [6]. World starch production currently exceeds 3,000 million metric tons [7] and is projected to double by 2050 to meet the nutritional needs of the growing world population [8].

Additionally, starch is utilized as a raw material in the industry. A breakthrough in nanotechnology has shown that incorporating nanoscale fillers into biopolymers to produce nanocomposites improves the biopolymer's properties. The nanoscale fillers have a huge surface area, which leads to a large interface between the polymer matrix and the fillers [9].

Zinc oxide (ZnO) is a semiconducting material whose research dates to the first quarter of the last century [10]. It belongs to the group of II-VI compounds with a broad direct bandgap ($E_g \sim 3.37$ eV) at room temperature [11]. During the past decade, the research interest in the nanostructures of ZnOhas been regenerated thanks to the synthesizing processes used. Several properties are obtained to produce ZnO. It has attracted the researcher's attention because of its properties and applications in sensors, electronics, and biomedical fields [12]. In addition, ZnO has a high exciton binding energy (60 meV), making it suitable for many industrial applications such as optoelectronic devices [13,14]. Also, ZnO contains many intrinsic and deep extrinsic impurities that emit light in various colors, including blue, green, purple, red, orange, and yellow [15,16]. Another area of interest relates to the length scale of ZnO nanoparticles. When the semiconductor's size is reduced to several nanometers, the quantum confinement effect occurs, altering its

optical properties. Starch is an ecofriendly renewable, abundant resource. It consists almost entirely of two major polysaccharides, namely amylose and amylopectin [17-19]. Recently, optical properties among other important parameters are correlated to the functionality of starch [20-21].

Graphene and its derivatives such as graphene oxide (GO), reduced graphene oxide (rGO) and graphene quantum dots (GQD) have been shown to be effective fillers in nanocomposites based on polymeric materials. The ideal dispersibility of graphene derivatives(GO, rGO and GQD) in the polymer matrix and their unique properties [22] can be utilized in many applications. For similar reasons, tuning of charges in the nanocomposites can be utilized to tune the molecule's selectivity to develop new membranes with superior properties [23,24]. Besides these unique properties, graphene also shows unique optical properties [25].

Therefore, this study aims to develop a simple method to fabricate starch/ZnO and starch/GO nanocomposites and characterize them optically. The overall aim is to control the effect of GO on the optical characteristics of starch/ZnO nanocomposite.

2. Materials and methods

2.1. Materials

All chemicals were used without any further purification. Zinc (II) acetate dihydrate (Fisher chemical, 99 %), Sodium hydroxide (Fisher Chemical, ≥ 97%). Graphite powder (Fisher Chemical), sulfuric acid (Scharlau, 96%), phosphoric acid (Fisher Chemical, 85%), potassium permanganate (Fisher Chemical, 99%), hydrogen peroxide (PioChem, 30%). Extra pure starch was acquired from Sisco Research Laboratories PVT.LTD, Bombay, India. Deionized (DI) Milli-Q water was used during this experiment.

2.2. ZnO Nanoparticles preparation

Zinc oxide nanoparticles were prepared using the co-precipitation method. In a typical method, a 100 ml of (1 M) zinc (II) acetatedehydrate was heated to 70°C, followed by dropwise addition of 2 M sodium hydroxide with stirring. After 1 hr, the precipitate was collected by centrifugation at 10000 rpm, washed several times with DI water, then dried in an oven

overnight at 80 °C, and finally calcined at 500 °C for 2 hr.

2.3. GO preparation

GO was prepared using the improved Hummers' method. A mixture of concentrated H_2SO_4/H_3PO_4 with a ratio of (9:1) was added to a mixture of 1 g graphite powder and 6 g $KMnO_4$ in an ice bath. The mixture was heated with stirring to 50 °C for 12 hrs. The mixture was cooled to 25 °C and added onto the ice with 1 ml of 30% H_2O_2. The precipitate was collected by centrifugation at 10000 rpm, washed the first time with 200 mL of 30% HCl, then washed several times with DI water, then dried in a vacuum oven overnight at room temperature.

2.4. Starch/ZnO nanocomposite preparation

50 ml of deionized water was heated using a magnetic stirrer at 100 ºC to dissolve starch. Then 0.5 gm of starch was added. After complete dissolution, the solution was stirred strongly for an additional 1 hr at 50 °C. Different weight percentages of ZnO nanoparticles were added to the starch solution (2, 4, 6, and 8 wt%) as presented in Table 1. The starch/ ZnO suspension was stirred for 1 hr. The homogeneous dispersion of ZnOwas accomplished by sonicating the prepared solutions for 2 hr. The solution was cast in plastic Petri dishes and left to dry in the air for 7 days.

3. Characterizing techniques

3.1. UV-Vis. measurement

UV-visible spectra of pure starch, starch/ZnO, and starch/GO were collected at room temperature in the 200–800 nm wavelength range, using a Jasco V-630 (Japan) spectrophotometer, Spectroscopy Department, National Research Centre, Cairo, Egypt.

4. Results and discussion

4.1. UV-Vis. results

To confirm the ZnO and GO nanoparticles' presence in the prepared nanocomposites, the UV–vis absorption spectra were recorded in the range of 200-800 nm, as depicted in Figure 1. As presented in the figure, a narrow absorption band centered at 368 nm for starch doped with different ZnO concentrations (2, 4, 6 and 8 wt%) attributed to ZnO NPs was observed, confirming the strong absorption of ZnO. The extinction peaks at 368 nm with varying intensity result from variations of the particle's size distribution. The absence of extinction peaks beyond 600 nm

(flattened spectrum) confirms that the reaction is saturated [26,27]. This may be since the reaction gets saturated and the reduction of Zn^{2+} to Zn^o is complete. The maximum absorption peak in the starch/GO spectrum appears at around 239 nm due to the π-π^* transition of GO [28].

4.2. Optical band gap results

The electron excitation from the lower energy level to the higher one is defined by the absorption edge, which can be estimated by extrapolation of the linear part of the absorption coefficient α with photon energy (hυ). The absorption coefficient can be determined using the following equation:

$$\alpha = (2.303 * A)/d \tag{1}$$

where A, and d are the absorbance and the thickness of prepared samples, respectively.

According to Tauc and Davis - Mott, the energy gap values and the type of electron transition between the valence and conduction bands can be determined using the following equation:

$$(\alpha h\upsilon)^r = B(h\upsilon\text{-}Eg), \tag{2}$$

Where hυ is the energy of the incident photons, B is a constant, and r is a constant that depends on the type of transition. The constant r takes values of 2,1/2, 2/3, and 1/3 if, for direct allowed transition, direct forbidden, indirect allowed, or indirect forbidden transition [29,30]. The bandgap energy was calculated using the equation of Eg (eV) = $h\upsilon$ = 1240/wavelength (nm), where Eg is the optical energy gap, h is Planck's constant, and c is the speed of light.

Figure 2 shows the estimated optical band gap of pure starch from the graph of both $(\alpha h\upsilon)^2$ and $(\alpha h\upsilon)^{1/2}$ versus the incident energy (hυ). The optical band gap energy (E_g) is estimated by extrapolating the linear portion of the curve to the axis of energy ($\alpha = 0$). The estimated direct allowed band gap value for pure starch was 2.58 and 5.67 eV, which means that pure starch has two optical absorption edges. Figure 3 presents the dependence of the starch optical band gap upon the filler concentration. Both $(\alpha h\upsilon)^2$ and $(\alpha h\upsilon)^{1/2}$ versus the incident energy are represented for starch/ZnO films in Figure 3. As presented in the last two figures, the prepared nanocomposites, in addition to pure starch, possess two absorption edges as two linear portions are present. Films of starch/ ZnO and starch/GO have two absorption shoulders and hence two band gaps [31]. However, for starch substituted

with GO (sample S6), the variation of $(\alpha h\nu)^2$ and $(\alpha h\nu)^{1/2}$ with the photon energy is depicted in Figure 4. The reduction of the starch optical bandgap due to substitution with ZnO and GO separately refers to the formation of defect levels within the valence band during the growth of the crystals, which is directly proportional to the ZnO and GO percentage. This causes the parabola of the density of state to extend to the absorption band edge [32]. The bandgap values are tabulated in Tables 2 and 3 for direct and indirect allowed transitions, respectively.

Table 2 shows that the bandgap values are decreased with increasing the filler concentration up to 6wt.% and decreased at higher levels. For indirect allowed transitions, the optical band gap is estimated by taking the value of r equals 1/2 in the Davis and Mott relation. Table 3 shows that increasing the ZnO concentration beyond 4wt.% causes the second absorption shoulder to disappear and hence the band gap to increase. This may be due to the aggregation of ions, which reduces mobility and conductivity. Since the values of the optical band gaps for allowed direct transition are higher than those of indirect ones, it was concluded that the transition type in starch/ZnO and starch/GO NPs is the direct transition, which reflects the crystallinity of the prepared films.

Table 1 Composition of starch/ZnO nanocomposites.

Sample	Starch (gm)	ZnO (gm)	GO(gm)
S1	0.50	0.00	0.00
S2	0.49	0.01	0.00
S3	0.48	0.02	0.00
S4	0.47	0.03	0.00
S5	0.46	0.04	0.00
S6	0.49	0.00	0.01

Table 2 Direct allowed optical band gap for pure starch, starch/ ZnO and starch/GO films.

Sample	E_{g1} (eV)	E_{g2}(eV)
S1	2.65	5.67
S2	3.21	5.21
S3	3.21	4.85
S4	3.18	3.38
S5	3.23	3.39
S6	1.99	5.24

Table 3 Indirect allowed optical band gap for pure starch, starch/ ZnO and starch/GO films.

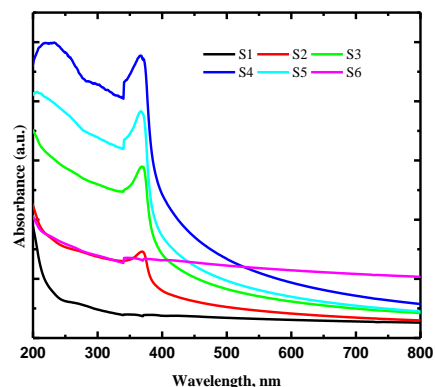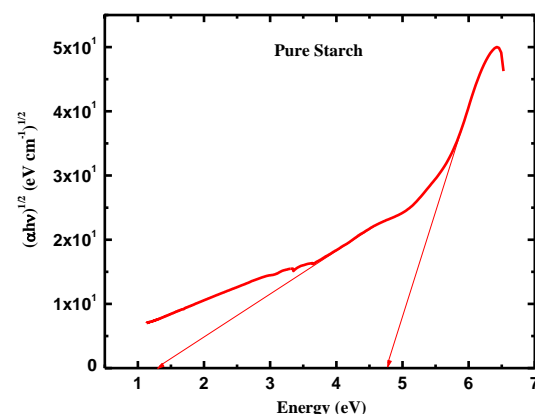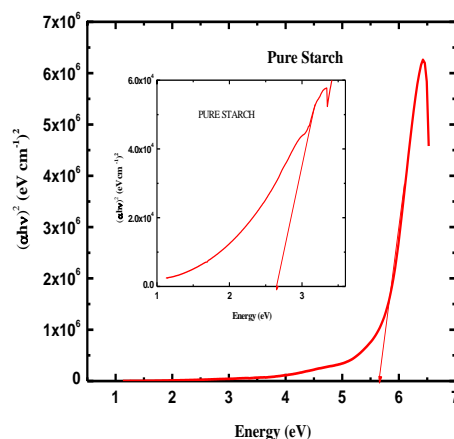| Sample	E_{g1}(eV)	E_{g2}(eV)
S1	1.33	4.77
S2	2.79	3.27
S3	1.25	2.94
S4	-	2.88
S5	-	3.04
S6	-	2.15

Fig. 1. UV–Vis absorption spectra of pristine starch (S1), starch with 2 wt.% of ZnO (S2), starch with 4 wt.% of ZnO (S3), starch with 6 wt.% of ZnO (S4), starch with 8.wt % of ZnO (S5), and starch with 2wt.% GO (S6).

(a)

Fig. 2. Variation of $(\alpha h\nu)^2$ and $(\alpha h\nu)^{1/2}$ with photon energy $(h\nu)$ for pure starch.
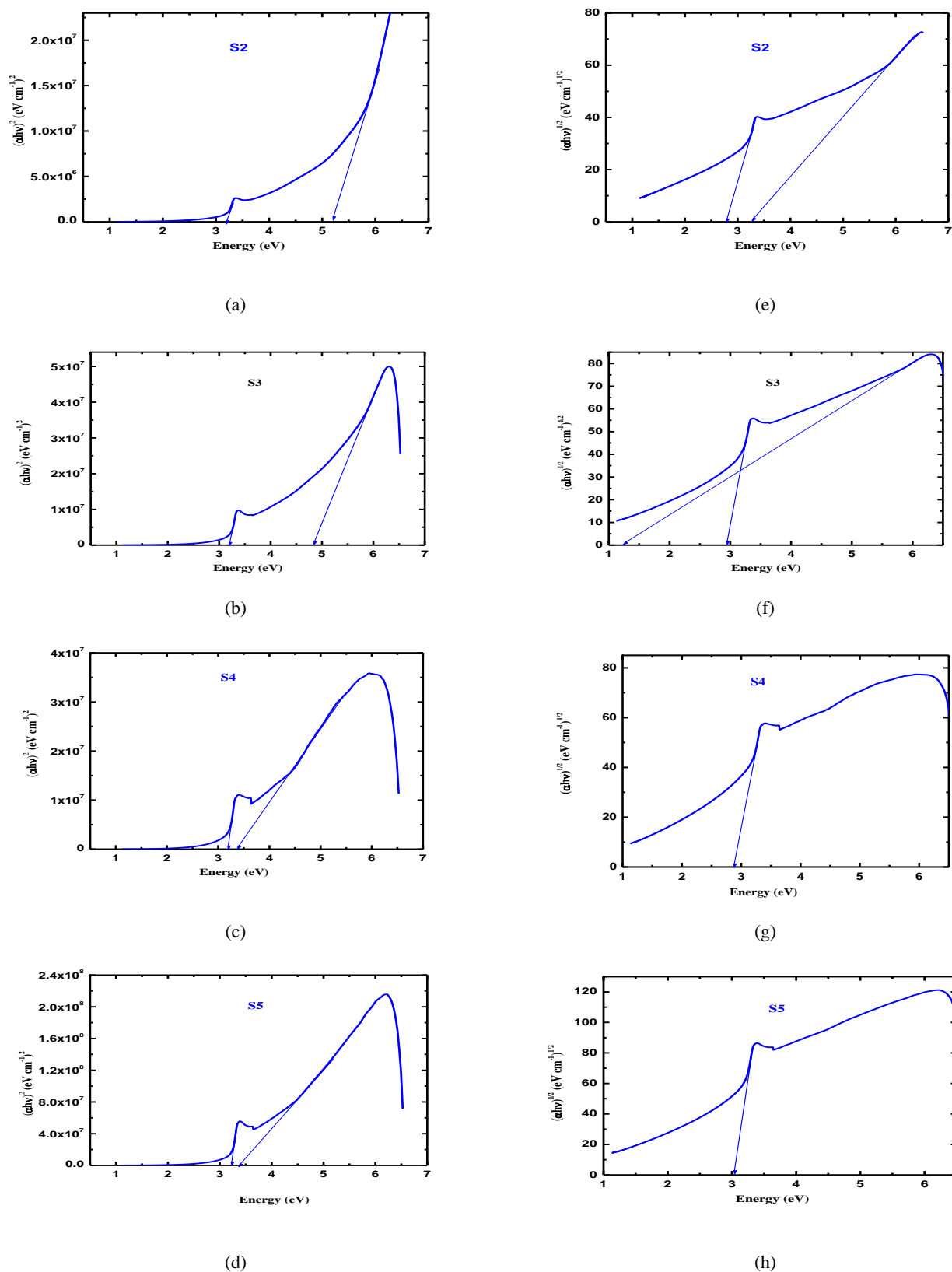
(a)

(b)

(c)

(d)

(e)

(f)

(g)

(h)

Fig. 3. Variation of $(\alpha h\upsilon)^2$ and $(\alpha h\upsilon)^{1/2}$ with photon energy ($h\upsilon$) for starch/ZnO with different concentrations of ZnO(2wt.% (sample S2), 4wt.% (sample S3), 6wt.% (sample S4) and 8wt.% (sample S5) respectively).
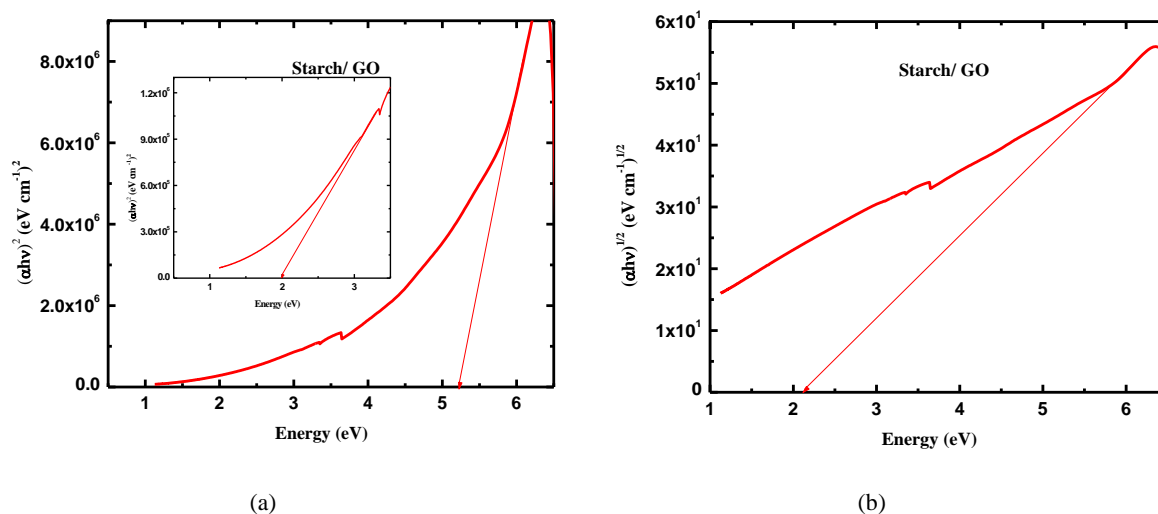
(a)   (b)

Fig. 4. Variation of $(\alpha h\upsilon)^2$ and $(\alpha h\upsilon)^{1/2}$ with photon energy (hυ) for starch / 2wt.% GO nanocomposites.

5. Conclusion

This work prepared a starch-based polymer nanocomposite with a small bandgap using the solution casting technique. The absorbance spectra for the nanocomposite films were recorded and showed a strong absorbance in the UV region of the electromagnetic spectrum. An absorption peak was observed at 368 nm for starch/ZnO films, attributed to ZnO nanoparticles. It was found that a relatively large

6. Conflicts of interest

Westate that "There are no conflicts to declare".

7. Formatting of funding sources

8. References

[1] Othan S.H., Kechik N.R.A., Shapi'i R.A., Talib R.A. and Tawakkal I.S.M.A., Water sorption and mechanical properties of starch/chitosan nanoparticle films. *J. Nanomater.* **2019**, 3843949, (2019).

[2] Singh P. and Sharma V.P., Integrated plastic waste management: Environmental and improved

shift from the absorption limit towards lower photonic energies is associated with the complexation between starch, ZnO, and GO. The starch has two direct and indirect optical band gaps, and they decreased due to the incorporation of ZnO NPs and GO. This reduction confirms the complexation between the starch chain and ZnO and GO, forming multiple trapping sites within the bandgap (i.e., between the valence and conduction bands).

health approaches. *Procedia Environ. Sci.***35**, 692–700, (2016).

[3] Ibrahim M.I.J., Sapuan S.M., Zainudin E.S. and Zuhri M.Y.M., Physical, thermal, morphological, and tensile properties of corn starch based films as affected by different plasticizers. *Int. J. Food Prop.,***22**, 925–941, (2019).

[4] Mograkar P. R. and Arfin T., Chemical and structural importance of starch based derivatives and its applications. *Natural polymers: derivatives, blends and composite. Nova Science Publishers, New York* (2017).

[5] Nasseri R. and Mohammadi N., Starch-based nanocomposites: A comparative performance study of cellulose whiskers and starch nanoparticles. *Carbohydrate polymers*, **106**, 432-439, (2014).

[6] Zeeman S. C., Kossmann J. and Smith A. M., Starch: its metabolism, evolution, and biotechnological modification in plants. *Annual review of plant biology*, **61**, 209-234, (2010).

[7] Fettke, J., Leifels, L., Brust, H., Herbst, K., &Steup, M. (2012). Two carbon fluxes to reserve

starch in potato (Solanumtuberosum L.) tuber cells are closely interconnected but differently modulated by temperature. *Journal of experimental botany*, *63*(8), 3011-3029.

[8] Tilman, D., Balzer, C., Hill, J., &Befort, B. L. (2011). Global food demand and the sustainable intensification of agriculture. *Proceedings of the national academy of sciences*, *108*(50), 20260-20264.

[9] Jamróz E., Kulawik P. and Kopel, P., The effect of nanofillers on the functional properties of biopolymer-based films: A review. *Polymers*, *11*(4), 675, (2019).

[10] Taghizadeh S. M., Lal N., Ebrahiminezhad A., Moeini F., Seifan M., Ghasemi Y. and Berenjian A., Green and economic fabrication of zinc oxide (ZnO) nanorods as a broadband UV blocker and antimicrobial agent. *Nanomaterials*, *10*(3), 530, (2020).

[11] Kumar R., Al-Dossary O., Kumar G. and Umar A., Zinc oxide nanostructures for NO 2 gas–sensor applications: A review. *Nano-Micro Letters*, *7*(2), 97-120, (2015).

[12] Leonardi S. G., Two-dimensional zinc oxide nanostructures for gas sensor applications. *Chemosensors*, *5*(2), 17, (2017).

[13] Chiu Y. H., Chang K. D. and Hsu Y. J., Plasmon-mediated charge dynamics and photoactivity enhancement for Au-decorated ZnO nanocrystals. *Journal of Materials Chemistry A*, *6*(10), 4286-4296, (2018).

[14] Huy N. N., Thuy V. T. T., Thang N. H., Thuy N. T., Khoi T. T. and Van Thanh D., Facile one-step synthesis of zinc oxide nanoparticles by ultrasonic-assisted precipitation method and its application for H2S adsorption in air. *Journal of Physics and Chemistry of Solids*, *132*, 99-103, (2019).

[15] Alghunaim N. S., Omar A., Elhaes H. and Ibrahim M., Effect of ZnO and TiO2 on the reactivity of some polymers. *Journal of Computational and Theoretical Nanoscience*, *14*(6), 2838-2843, (2017).

[16] Badry R., Fahmy A., Ibrahim A., Elhaes H. and Ibrahim M., Application of polyvinyl alcohol/polypropylene/zinc oxide nanocomposites as sensor: modeling approach. *Optical and Quantum Electronics*, *53*(1), 1-12, (2021).

[17] Kim S.R.B. , Choi Y., Kim J. and Lim S., Improvement of water solubility and humidity stability of tapioca starch film by incorporating various gums, LWT – *Food Science and Technology*, *64* (1), 475-482, (2015).

[18] Gelders G.G. Vanderstukken T.C., Goesaert H. and Delcour J.A., Amylose–lipidcomplexation: A new fractionation method, *Carbohydrate Polymers*, *56* (4), 447-458, (2004).

[19] Sapper M., Talens P. and Chiralt A., Improving functional properties of cassava starch-based films by incorporating xanthan, gellan, or pullulan gums.*International Journal of Polymer Science*, *2019* ,1-8, (2019).

[20] Wang B., Yan S., Gao W., Kang X., Yu B., Liu P., Guo L., Cui B. andAbd El-Aty A.M., Antibacterial activity, optical, and functional properties of corn starch-based films impregnated with bamboo leaf volatile oil, *Food Chemistry*, *357*, 129743, (2021).

[21] Darmawan Z. T., Heryanto H., Mutmainna I., Abdullah B. and Tahir D., Effect of Magnesium (Mg) to the Optical and Absorption Gamma-Ray Properties of Composite Shield Cassava Starch /Fe3O4/Mg, *Radiation Physics and Chemistry*, *191*, 109843, (2022).

[22] Smith A. T., LaChance A. M., Zeng S., Liu B. and Sun, L., Synthesis, properties, and applications of graphene oxide/reduced graphene oxide and their nanocomposites. *Nano Materials Science*, *1*(1), 31-47, (2019).

[23] Tan B. and Thomas N. L., A review of the water barrier properties of polymer/clay and polymer/graphene nanocomposites. *Journal of Membrane Science*, *514*, 595-612, (2016).

[24] Cheng C., Li S., Thomas A., Kotov N. A. and Haag R. Functional graphene nanomaterials based architectures: biointeractions, fabrications, and emerging biological applications. *Chemical reviews*, *117*(3), 1826-1914, (2017).

[25] Ojrzynska M., Wroblewska A., Judek J., Malolepszy A., Duzynska A. and Zdrojek M.,Study of optical properties of graphene flakes and its derivatives in aqueous solutions.*Optics Express,* *28*, 7274-7281 (2020).

[26] Menchaca-Rivera J. A., Gonzalez-Reyna M. A., Avilés-Arellano L. M., Fernández-Loyola R., Morales-Sánchez E. and Pérez Robles J. F., Determination of optical properties of a corn starch biofilm. *Journal of Applied Polymer Science*, *136*(9), 47111 (2019).

[27] Chowdhury T. and Das, M., Effect of antimicrobial on mechanical, barrier and optical properties of corn starch based self-supporting edible film. *International Journal of Food Studies*, 2(2), (2013).

[28] Gangwar P., Singh S. and Khare, N., Study of optical properties of graphene oxide and its derivatives using spectroscopic ellipsometry. *Applied Physics A*, *124* (9), 1-8, (2018).

[29] Badry R., Ezzat H. A., El-Khodary S., Morsy M., Elhaes H., Nada N. and Ibrahim M., Spectroscopic and thermal analyses for the effect

of acetic acid on the plasticized sodium carboxymethyl cellulose. *Journal of Molecular Structure*, **1224**, 129013 (2021).

[30] Badry R., El-Khodary S., Elhaes H., Nada N. and Ibrahim, M., Optical, conductivity and dielectric properties of plasticized solid polymer electrolytes based on blends of sodium carboxymethyl cellulose and polyethylene

oxide. *Optical and Quantum Electronics*, **53**(1), 1-15 (2021).

[31] Elkomy G. M., Mousa S. M. and Mostafa H. A., Structural and optical properties of pure PVA/PPY and cobalt chloride doped PVA/PPY films. *Arabian Journal of Chemistry*, **9**, S1786-S1792 (2016).

[32] Murri R., Schiavulli L., Pinto N. and Ligonzo T., Urbach tail in amorphous gallium arsenide films. *Journal of non-crystalline solids*, **139**, 60-66 (1992).